Vision-Based Defect Inspection for Sewer Pipes

Subjects: Engineering, Civil

Contributor: Hanxiang Wang, YANFEN LI, L. Minh Dang, SONG Hyoung-Kyu, Hyeonjoon Moon

Underground sewerage systems (USSs) are a vital part of public infrastructure that contributes to collecting wastewater or stormwater from various sources and conveying it to storage tanks or sewer treatment facilities. A healthy USS with proper functionality can effectively prevent urban waterlogging and play a positive role in the sustainable development of water resources. Since it was first introduced in the 1960s, computer vision (CV) has become a mature technology that is used to realize promising automation for sewer inspections.

Keywords: survey ; computer vision ; defect inspection ; condition assessment ; sewer pipes

1. Introduction

1.1. Background

Underground sewerage systems (USSs) are a vital part of public infrastructure that contributes to collecting wastewater or stormwater from various sources and conveying it to storage tanks or sewer treatment facilities. A healthy USS with proper functionality can effectively prevent urban waterlogging and play a positive role in the sustainable development of water resources. However, sewer defects caused by different influence factors such as age and material directly affect the degradation of pipeline conditions. It was reported in previous studies that the conditions of USSs in some places are unsatisfactory and deteriorate over time. For example, a considerable proportion (20.8%) of Canadian sewers is graded as poor and very poor. The rehabilitation of these USSs is needed in the following decade in order to ensure normal operations and services on a continuing basis [1]. Currently, the maintenance and management of USSs have become challenging problems for municipalities worldwide due to the huge economic costs [2]. In 2019, a report in the United States of America (USA) estimated that utilities spent more than USD 3 billion on wastewater pipe replacements and repairs, which addressed 4692 miles of pipeline [3].

1.2. Defect Inspection Framework

Since it was first introduced in the 1960s [4], computer vision (CV) has become a mature technology that is used to realize promising automation for sewer inspections. In order to meet the increasing demands on USSs, a CV-based defect inspection system is required to identify, locate, or segment the varied defects prior to the rehabilitation process. As illustrated in **Figure 1**, an efficient defect inspection framework for underground sewer pipelines should cover five stages. In the data acquisition stage, there are many available techniques such as closed-circuit television (CCTV), sewer scanner and evaluation technology (SSET), and totally integrated sonar and camera systems (TISCITs) [5]. CCTV-based inspections rely on a remotely controlled tractor or robot with a mounted CCTV camera [6]. An SSET is a type of method that acquires the scanned data from a suite of sensor devices [7]. The TISCIT system utilizes sonar and CCTV cameras to obtain a 360° view of the sewer conditions [5]. As mentioned in several studies [6][8][9][10], CCTV-based inspections are the most widely used methods due to the advantages of economics, safety, and simplicity. Nevertheless, the performance of CCTV-based inspections is limited by the quality of the acquired data. Therefore, image-based learning methods require pre-processing algorithms to remove noise and enhance the resolution of the collected images. Many studies on sewer inspections have recently applied image pre-processing before examining the defects [11][12][13].

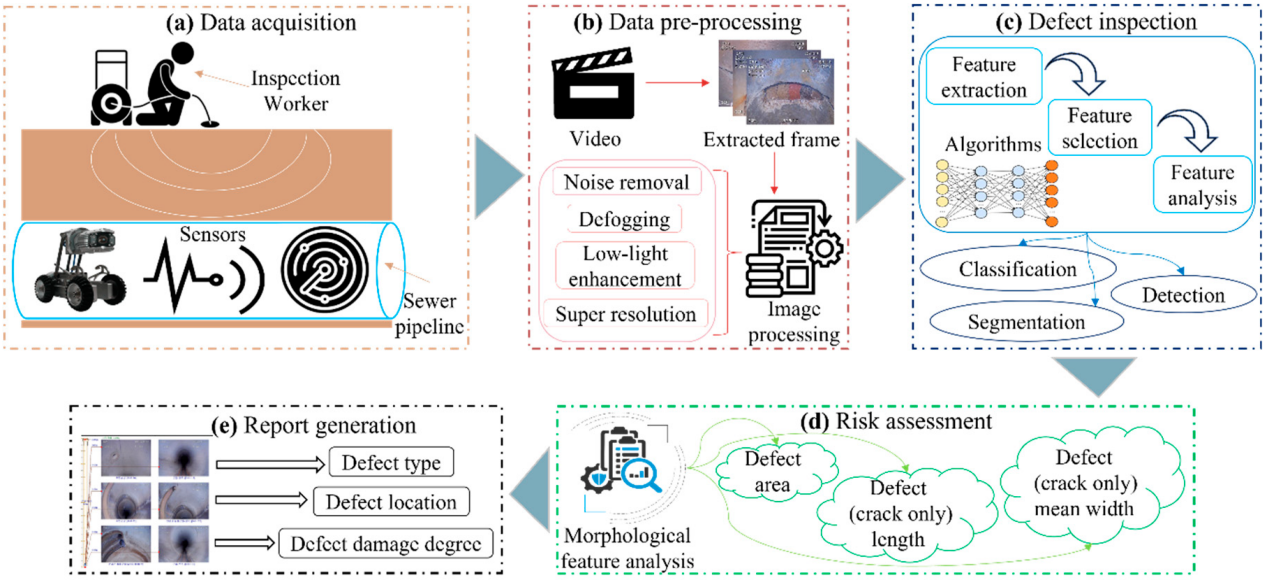

Figure 1. There are five stages in the defect inspection framework, which include (**a**) the data acquisition stage based on various sensors (CCTV, sonar, or scanner), (**b**) the data processing stage for the collected data, (**c**) the defect inspection stage containing different algorithms (defect classification, detection, and segmentation), (**d**) the risk assessment for detected defects using image post-processing, and (**e**) the final report generation stage for the condition evaluation.

2. Defect Inspection

In this section, several classic algorithms are illustrated, and the research tendency is analyzed. **Figure 2** provides a brief description of the algorithms in each category. In order to comprehensively analyze these studies, the publication time, title, utilized methodology, advantages, and disadvantages for each study are covered. Moreover, the specific proportion of each inspection algorithm is computed in **Figure 3**. It is clear that the defect classification accounts for the most significant percentages in all the investigated studies.

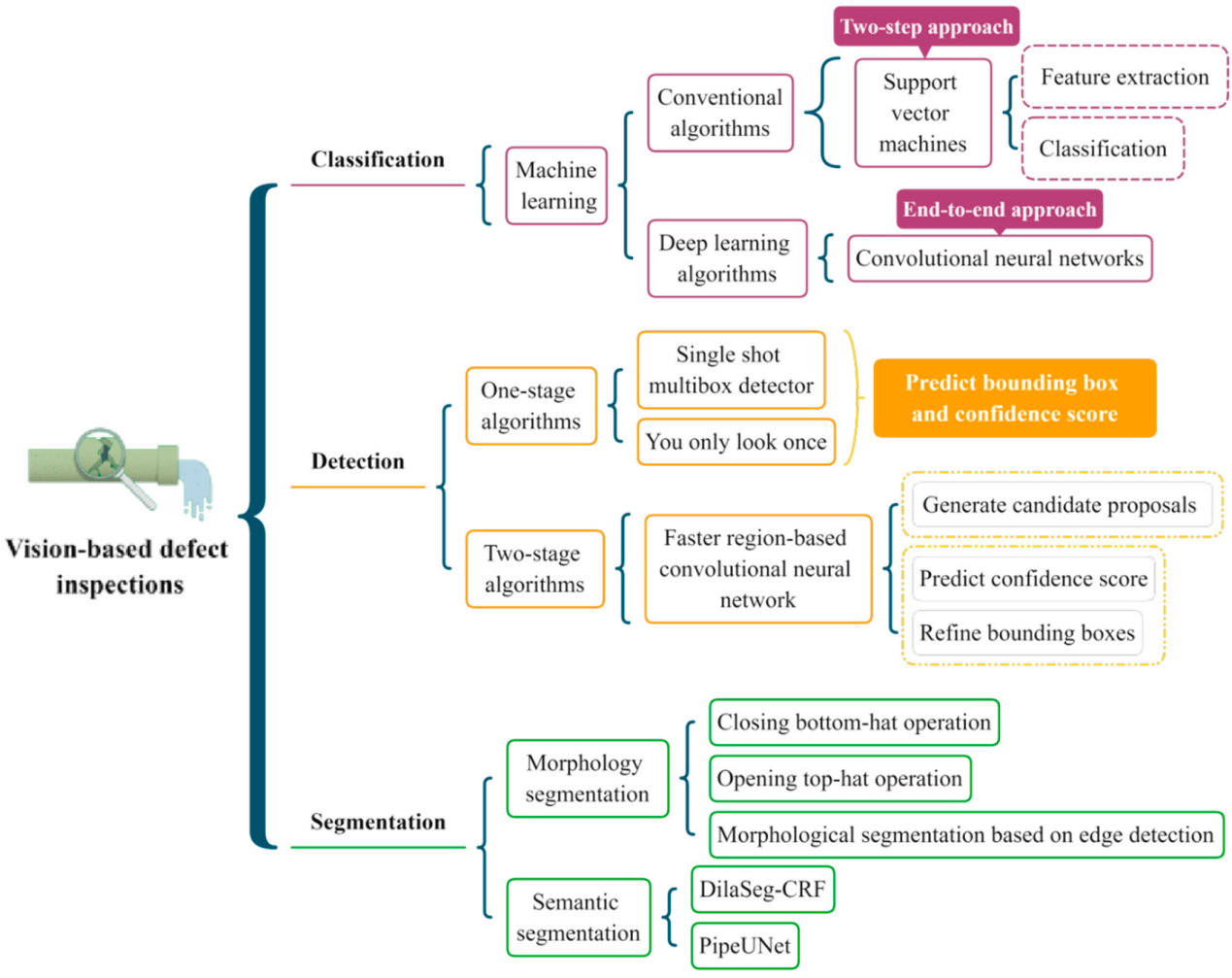

Figure 2. The classification map of the existing algorithms for each category. The dotted boxes represent the main stages of the algorithms.

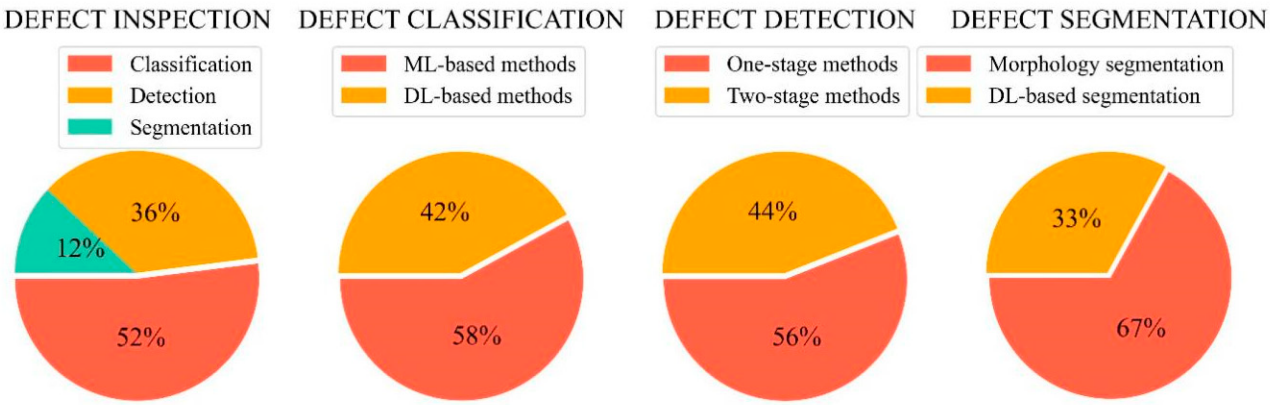

Figure 3. Proportions of the investigated studies using different inspection algorithms.

2.1. Defect Classification

Due to the recent advancements in ML, both the scientific community and industry have attempted to apply ML-based pattern recognition in various areas, such as agriculture [14], resource management [15], and construction [16]. At present, many types of defect classification algorithms have been presented for both binary and multi-class classification tasks.

2.2. Defect Detection

Rather than the classification algorithms that merely offer each defect a class type, object detection is conducted to locate and classify the objects among the predefined classes using rectangular bounding boxes (BBs) as well as confidence scores (CSs). In recent studies, object detection technology has been increasingly applied in several fields, such as intelligent transportation [17][18][19], smart agriculture [20][21][22], and autonomous construction [23][24][25]. The generic object detection consists of the one-stage approaches and the two-stage approaches. The classic one-stage detectors based on regression include YOLO [26], SSD [27], CornerNet [28], and RetinaNet [29]. The two-stage detectors are based on region proposals, including Fast R-CNN [30], Faster R-CNN [31], and R-FCN [32].

2.3. Defect Segmentation

Defect segmentation algorithms can predict defect categories and pixel-level location information with exact shapes, which is becoming increasingly significant for the research on sewer condition assessment by re-coding the exact defect attributes and analyzing the specific severity of each defect. The previous segmentation methods were mainly based on mathematical morphology [33][34]. However, the morphology segmentation approaches were inefficient compared to the DL-based segmentation methods. As a result, the defect segmentation methods based on DL have been recently explored in various fields.

3. Dataset and Evaluation Metric

The performances of all the algorithms were tested and are reported based on a specific dataset using specific metrics. As a result, datasets and protocols were two primary determining factors in the algorithm evaluation process. The evaluation results are not convincing if the dataset is not representative, or the used metric is poor. It is challenging to judge what method is the SOTA because the existing methods in sewer inspections utilize different datasets and protocols. Therefore, benchmark datasets and standard evaluation protocols are necessary to be provided for future studies.

3.1. Dataset

3.1.1. Dataset Collection

Currently, many data collection robotic systems have emerged that are capable of assisting workers with sewer inspection and spot repair. **Table 1** lists the latest advanced robots along with their respective information, including the robot's name, company, pipe diameter, camera feature, country, and main strong points. **Figure 4** introduces several representative robots that are widely utilized to acquire images or videos from underground infrastructures. As shown in **Figure 4**a, LETS 6.0 is a versatile and powerful inspection system that can be quickly set up to operate in 150 mm or

larger pipes. A representative work (Robocam 6) of the Korean company TAP Electronics is shown in **Figure 4**b. Robocam 6 is the best model to increase the inspection performance without the considerable cost of replacing the equipment. **Figure 4**c is the X5-HS robot that was developed in China, which is a typical robotic crawler with a high-definition camera. In **Figure 4**d, Robocam 3000, sold by Japan, is the only large-scale system that is specially devised for inspecting pipes ranging from 250 mm to 3000 mm. It used to be unrealistic to apply the crawler in huge pipelines in Korea.

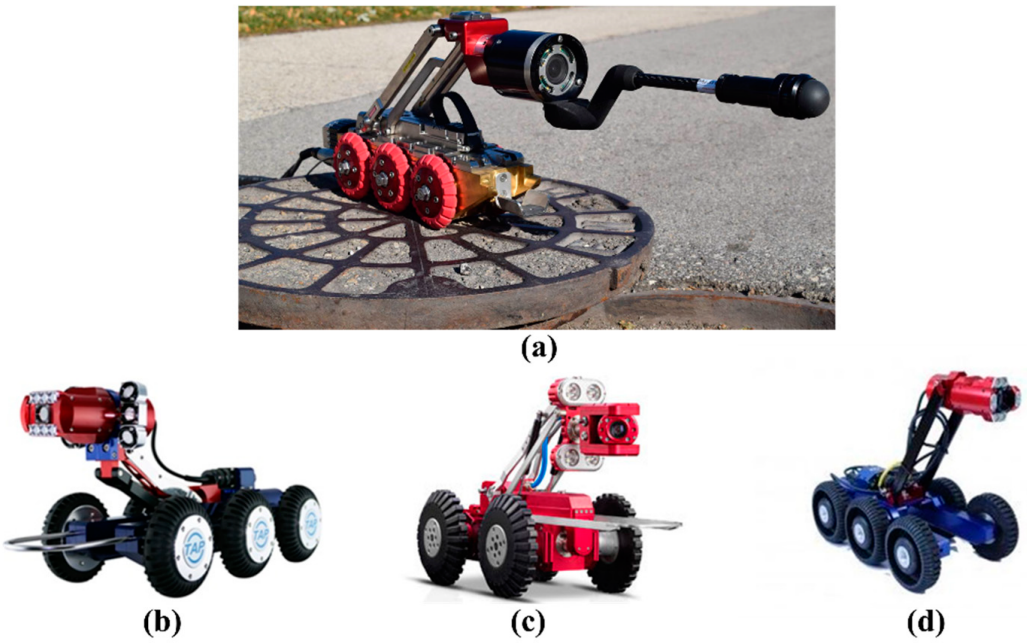

Figure 4. Representative inspection robots for data acquisition. (**a**) LETS 6.0, (**b**) Robocam 6, (**c**) X5-HS, and (**d**) Robocam 3000.

Table 1. The detailed information of the latest robots for sewer inspection.

Name	Company	Pipe Diameter	Camera Feature	Country	Strong Point
CAM160 (https://goolnk.com/YrYQob accessed on 20 February 2022)	Sewer Robotics	200–500 mm	NA	USA	● Auto horizon adjustment ● Intensity adjustable LED lighting ● Multifunctional
LETS 6.0 (https://ariesindustries.com/products/ accessed on 20 February 2022)	ARIES INDUSTRIES	150 mm or larger	Self-leveling lateral camera or a Pan and tilt camera	USA	● Slim tractor profile ● Superior lateral camera ● Simultaneously acquire mainline and lateral videos

Name	Company	Pipe Diameter	Camera Feature	Country	Strong Point
wolverine® 2.02	ARIES INDUSTRIES	150–450 mm	NA	USA	● Powerful crawler to maneuver obstacles ● Minimum set uptime ● Camera with lens cleaning technique
X5-HS (https://goolnk.com/Rym02W accessed on 20 February 2022)	EASY-SIGHT	300–3000 mm	≥2 million pixels	China	● High-definition ● Freely choose wireless and wired connection and control ● Display and save videos in real time
Robocam 6 (https://goolnk.com/43pdGA accessed on 20 February 2022)	TAP Electronics	600 mm or more	Sony 130-megapixel Exmor 1/3-inch CMOS	Korea	● High-resolution ● All-in-one subtitle system
RoboCam Innovation4	TAP Electronics	600 mm or more	Sony 130-megapixel Exmor 1/3-inch CMOS	Korea	● Best digital record performance ● Super white LED lighting ● Cableless
Robocam 30004	TAP Electronics' Japanese subsidiary	250–3000 mm	Sony 1.3-megapixel Exmor CMOS color	Japan	● Can be utilized in huge pipelines ● Optical 10X zoom performance

3.1.2. Benchmarked Dataset

Open-source sewer defect data is necessary for academia to promote fair comparisons in automatic multi-defect classification tasks. In this survey, a publicly available benchmark dataset called Sewer-ML [35] for vision-based defect classification is introduced. The Sewer-ML dataset, acquired from Danish companies, contains 1.3 million images labeled by sewer experts with rich experience. **Figure 5** shows some sample images from the Sewer-ML dataset, and each image includes one or more classes of defects. The recorded text in the image was redacted using a Gaussian blur kernel to protect private information. Besides, the detailed information of the datasets used in recent papers is described in **Table 2**. This research summarizes 32 datasets from different countries in the world, of which the USA has 12 datasets, accounting for the largest proportion. The largest dataset contains 2,202,582 images, whereas the smallest dataset has only 32

images. Since the images were acquired by various types of equipment, the collected images have varied resolutions ranging from 64 × 64 to 4000 × 46,000.

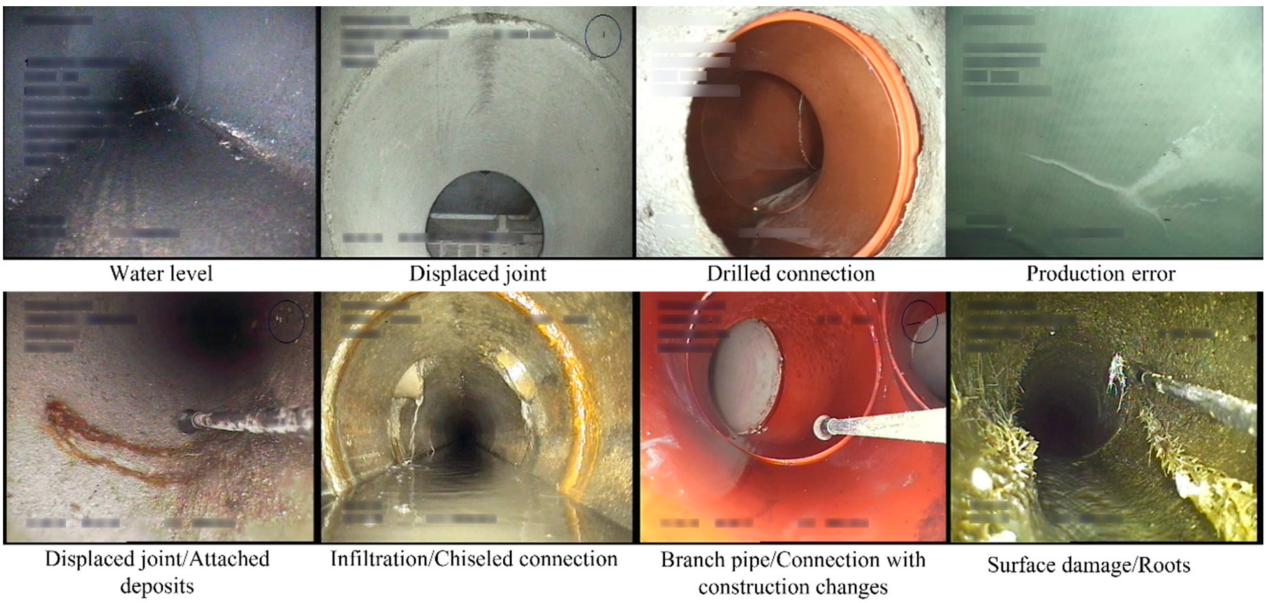

Figure 5. Sample images from the Sewer-ML dataset that has a wide diversity of materials and shapes.

Table 2. Research datasets for sewer defects in recent studies.

ID	Defect Type	Image Resolution	Equipment	Number of Images	Country	Ref.
1	Broken, crack, deposit, fracture, hole, root, tap	NA	NA	4056	Canada	[9]
2	Connection, crack, debris, deposit, infiltration, material change, normal, root	1440 × 720–320 × 256	RedZone® Solo CCTV crawler	12,000	USA	[36]
3	Attached deposit, defective connection, displaced joint, fissure, infiltration, ingress, intruding connection, porous, root, sealing, settled deposit, surface	1040 × 1040	Front-facing and back-facing camera with a 185∘ wide lens	2,202,582	The Netherlands	[37]
4	Dataset 1: defective, normal Dataset 2: barrier, deposit, disjunction, fracture, stagger, water	NA	NA	40,000 15,000	China	[38]
5	Broken, deformation, deposit, other, joint offset, normal, obstacle, water	1435 × 1054–296 × 166	NA	18,333	China	[39]
6	Attached deposits, collapse, deformation, displaced joint, infiltration, joint damage, settled deposit	NA	NA	1045	China	[40]

ID	Defect Type	Image Resolution	Equipment	Number of Images	Country	Ref.
7	Circumferential crack, longitudinal crack, multiple crack	320 × 240	NA	335	USA	[11]
8	Debris, joint faulty, joint open, longitudinal, protruding, surface	NA	Robo Cam 6 with a 1/3-in. SONY Exmor CMOS camera	48,274	South Korea	[41]
9	Broken, crack, debris, joint faulty, joint open, normal, protruding, surface	1280 × 720	Robo Cam 6 with a megapixel Exmor CMOS sensor	115,170	South Korea	[42]
10	Crack, deposit, else, infiltration, joint, root, surface	NA	Remote cameras	2424	UK	[43]
11	Broken, crack, deposit, fracture, hole, root, tap	NA	NA	1451	Canada	[44]
12	Crack, deposit, infiltration, root	1440 × 720–320 × 256	RedZone® Solo CCTV crawler	3000	USA	[45]
13	Connection, fracture, root	1507 × 720–720 × 576	Front facing CCTV cameras	3600	USA	[46]
14	Crack, deposit, root	928 × 576–352 × 256	NA	3000	USA	[47]
15	Crack, deposit, root	512 × 256	NA	1880	USA	[48]
16	Crack, infiltration, joint, protruding	1073 × 749–296 × 237	NA	1106	China	[49]
17	Crack, non-crack	64 × 64	NA	40,810	Australia	[50]
18	Crack, normal, spalling	4000 × 46,000–3168 × 4752	Canon EOS. Tripods and stabilizers	294	China	[51]
19	Collapse, crack, root	NA	SSET system	239	USA	[52]
20	Clean pipe, collapsed pipe, eroded joint, eroded lateral, misaligned joint, perfect joint, perfect lateral	NA	SSET system	500	USA	[53]
21	Cracks, joint, reduction, spalling	512 × 512	CCTV or Aqua Zoom camera	1096	Canada	[54]

ID	Defect Type	Image Resolution	Equipment	Number of Images	Country	Ref.
22	Defective, normal	NA	CCTV (Fisheye)	192	USA	[55]
23	Deposits, normal, root	1507 × 720–720 × 576	Front-facing CCTV cameras	3800	USA	[56]
24	Crack, non-crack	240 × 320	CCTV	200	South Korea	[57]
25	Faulty, normal	NA	CCTV	8000	UK	[58]
26	Blur, deposition, intrusion, obstacle	NA	CCTV	12,000	NA	[59]
27	Crack, deposit, displaced joint, ovality	NA	CCTV (Fisheye)	32	Qatar	[60]
29	Crack, non-crack	320 × 240–20 × 20	CCTV	100	NA	[61]
30	Barrier, deposition, distortion, fraction, inserted	600 × 480	CCTV and quick-view (QV) cameras	10,000	China	[62]
31	Fracture	NA	CCTV	2100	USA	[63]
32	Broken, crack, fracture, joint open	NA	CCTV	291	China	[64]

3.2. Evaluation Metric

The studied performances are ambiguous and unreliable if there is no suitable metric. In order to present a comprehensive evaluation, multitudinous methods are proposed in recent studies. Detailed descriptions of different evaluation metrics are explained in **Table 3**. **Table 4** presents the performances of the investigated algorithms on different datasets in terms of different metrics.

Table 3. Overview of the evaluation metrics in the recent studies.

Metric	Description	Ref.
Precision	The proportion of positive samples in all positive prediction samples	[9]
Recall	The proportion of positive prediction samples in all positive samples	[36]
Accuracy	The proportion of correct prediction in all prediction samples	[36]
F1-score	Harmonic mean of precision and recall	[38]
FAR	False alarm rate in all prediction samples	[55]
True accuracy	The proportion of all predictions excluding the missed defective images among the entire actual images	[65]

Metric	Description	Ref.
AUROC	Area under the receiver operator characteristic (ROC) curve	[37]
AUPR	Area under the precision-recall curve	[37]
mAP	mAP first calculates the average precision values for different recall values for one class, and then takes the average of all classes	[9]
Detection rate	The ratio of the number of the detected defects to total number of defects	[57]
Error rate	The ratio of the number of mistakenly detected defects to the number of non-defects	[57]
PA	Pixel accuracy calculating the overall accuracy of all pixels in the image	[48]
mPA	The average of pixel accuracy for all categories	[48]
mIoU	The ratio of intersection and union between predictions and GTs	[48]
fwIoU	Frequency-weighted IoU measuring the mean IoU value weighing the pixel frequency of each class	[48]

Table 4. Performances of different algorithms in terms of different evaluation metrics.

ID	Number of Images	Algorithm	Task	Performance		Ref.
				Accuracy (%)	Processing Speed	
1	3 classes	Multiple binary CNNs	Classification	Accuracy: 86.2 Precision: 87.7 Recall: 90.6	NA	[36]
2	12 classes	Single CNN	Classification	AUROC: 87.1 AUPR: 6.8	NA	[36]

ID	Number of Images	Algorithm	Task	Performance		Ref.
				Accuracy (%)	Processing Speed	
3	Dataset 1: 2 classes Dataset 2: 6 classes	Two-level hierarchical CNNs	Classification	Accuracy: 94.5 Precision: 96.84 Recall: 92 F1-score: 94.36 Accuracy: 94.96 Precision: 85.13 Recall: 84.61 F1-score: 84.86	1.109 h for 200 videos	[38]
4	8 classes	Deep CNN	Classification	Accuracy: 64.8	NA	[39]
5	6 classes	CNN	Classification	Accuracy: 96.58	NA	[41]
6	8 classes	CNN	Classification	Accuracy: 97.6	0.15 s/image	[42]
7	7 classes	Multi-class random forest	Classification	Accuracy: 71	25 FPS	[43]
8	7 classes	SVM	Classification	Accuracy: 84.1	NA	[40]
9	3 classes	SVM	Classification	Recall: 90.3 Precision: 90.3	10 FPS	[11]
10	3 classes	CNN	Classification	Accuracy: 96.7 Precision: 99.8 Recall: 93.6 F1-score: 96.6	15 min 30 images	[51]
11	3 classes	RotBoost and statistical feature vector	Classification	Accuracy: 89.96	1.5 s/image	[52]
12	7 classes	Neuro-fuzzy classifier	Classification	Accuracy: 91.36	NA	[53]
13	4 classes	Multi-layer perceptions	Classification	Accuracy: 98.2	NA	[54]
14	2 classes	Rule-based classifier	Classification	Accuracy: 87 FAR: 18 Recall: 89	NA	[55]

ID	Number of Images	Algorithm	Task	Performance		Ref.
				Accuracy (%)	Processing Speed	
15	2 classes	OCSVM	Classification	Accuracy: 75	NA	[58]
16	4 classes	CNN	Classification	Recall: 88 Precision: 84 Accuracy: 85	NA	[59]
17	2 class	Rule-based classifier	Classification	Accuracy: 84 FAR: 21 True accuracy: 95	NA	[65]
18	4 classes	RBN	Classification	Accuracy: 95	NA	[64]
19	7 classes	YOLOv3	Detection	mAP: 85.37	33 FPS	[9]
20	4 classes	Faster R-CNN	Detection	mAP: 83	9 FPS	[45]
21	3 classes	Faster R-CNN	Detection	mAP: 77	110 ms/image	[46]
22	3 classes	Faster R-CNN	Detection	Precision: 88.99 Recall: 87.96 F1-score: 88.21	110 ms/image	[47]
23	2 classes	CNN	Detection	Accuracy: 96 Precision: 90	0.2782 s/image	[50]
24	3 classes	Faster R-CNN	Detection	mAP: 71.8	110 ms/image	[63]
		SSD		mAP: 69.5	57 ms/image	
		YOLOv3		mAP: 53	33 ms/image	
25	2 classes	Rule-based detector	Detection	Detection rate: 89.2 Error rate: 4.44	1 FPS	[57]
26	2 classes	GA and CNN	Detection	Detection rate: 92.3	NA	[61]
27	5 classes	SRPN	Detection	mAP: 50.8 Recall: 82.4	153 ms/image	[62]

ID	Number of Images	Algorithm	Task	Performance		Ref.
				Accuracy (%)	Processing Speed	
28	1 class	CNN and YOLOv3	Detection	AP: 71	65 ms/image	[66]
29	3 classes	DilaSeg-CRF	Segmentation	PA: 98.69 mPA: 91.57 mIoU: 84.85 fwIoU: 97.47	107 ms/image	[48]
30	4 classes	PipeUNet	Segmentation	mIoU: 76.37	32 FPS	[49]

As shown in **Table 4**, accuracy is the most commonly used metric in the classification tasks [36][38][39][40][41][42][43][51][52][53][54][55][58][59][65]. In addition to this, other subsidiary metrics such as precision [11][36][38][51][59], recall [11][36][38][51][55][59], and F1-score [38][51] are also well supported. Furthermore, AUROC and AUPR are calculated in [37] to measure the classification results, and FAR is used in [55][65] to check the false alarm rate in all the predictions. In contrast to classification, mAP is a principal metric for detection tasks [9][45][46][62][63]. In another study [47], precision, recall, and F1-score are reported in conjunction to provide a comprehensive estimation for defect detection. Heo et al. [57] assessed the model performance based on the detection rate and the error rate. Kumar and Abraham [66] report the average precision (AP), which is similar to the mAP but for each class. For the segmentation tasks, the mIoU is considered as an important metric that is used in many studies [48][49]. Apart from the mIoU, the per-class pixel accuracy (PA), mean pixel accuracy (mPA), and frequency-weighted IoU (fwIoU) are applied to evaluate the segmented results at the pixel level.

References

1. The 2019 Canadian Infrastructure Report Card (CIRC). 2019. Available online: http://canadianinfrastructure.ca/downloads/canadian-infrastructure-report-card-2019.pdf (accessed on 20 February 2022).
2. Tscheikner-Gratl, F.; Caradot, N.; Cherqui, F.; Leitão, J.P.; Ahmadi, M.; Langeveld, J.G.; Le Gat, Y.; Scholten, L.; Roghani, B.; Rodríguez, J.P.; et al. Sewer asset management–state of the art and research needs. Urban Water J. 2019, 16, 662–675.
3. 2021 Report Card for America's Infrastructure 2021 Wastewater. Available online: https://infrastructurereportcard.org/wp-content/uploads/2020/12/Wastewater-2021.pdf (accessed on 20 February 2022).
4. Spencer, B.F., Jr.; Hoskere, V.; Narazaki, Y. Advances in computer vision-based civil infrastructure inspection and monitoring. Engineering 2019, 5, 199–222.
5. Duran, O.; Althoefer, K.; Seneviratne, L.D. State of the art in sensor technologies for sewer inspection. IEEE Sens. J. 2002, 2, 73–81.
6. 2021 Global Green Growth Institute. 2021. Available online: http://gggi.org/site/assets/uploads/2019/01/Wastewater-System-Operation-and-Maintenance-Guideline-1.pdf (accessed on 20 February 2022).
7. Haurum, J.B.; Moeslund, T.B. A Survey on image-based automation of CCTV and SSET sewer inspections. Autom. Constr. 2020, 111, 103061.
8. Mostafa, K.; Hegazy, T. Review of image-based analysis and applications in construction. Autom. Constr. 2021, 122, 103516.
9. Yin, X.; Chen, Y.; Bouferguene, A.; Zaman, H.; Al-Hussein, M.; Kurach, L. A deep learning-based framework for an automated defect detection system for sewer pipes. Autom. Constr. 2020, 109, 102967.
10. Czimmermann, T.; Ciuti, G.; Milazzo, M.; Chiurazzi, M.; Roccella, S.; Oddo, C.M.; Dario, P. Visual-based defect detection and classification approaches for industrial applications—A survey. Sensors 2020, 20, 1459.
11. Zuo, X.; Dai, B.; Shan, Y.; Shen, J.; Hu, C.; Huang, S. Classifying cracks at sub-class level in closed circuit television sewer inspection videos. Autom. Constr. 2020, 118, 103289.

12. Dang, L.M.; Hassan, S.I.; Im, S.; Mehmood, I.; Moon, H. Utilizing text recognition for the defects extraction in sewers C CTV inspection videos. Comput. Ind. 2018, 99, 96–109.

13. Li, C.; Lan, H.-Q.; Sun, Y.-N.; Wang, J.-Q. Detection algorithm of defects on polyethylene gas pipe using image recognit ion. Int. J. Press. Vessel. Pip. 2021, 191, 104381.

14. Li, Y.; Wang, H.; Dang, L.M.; Sadeghi-Niaraki, A.; Moon, H. Crop pest recognition in natural scenes using convolutional neural networks. Comput. Electron. Agric. 2020, 169, 105174.

15. Wang, H.; Li, Y.; Dang, L.M.; Ko, J.; Han, D.; Moon, H. Smartphone-based bulky waste classification using convolutiona l neural networks. Multimed. Tools Appl. 2020, 79, 29411–29431.

16. Hassan, S.I.; Dang, L.-M.; Im, S.-H.; Min, K.-B.; Nam, J.-Y.; Moon, H.-J. Damage Detection and Classification System f or Sewer Inspection using Convolutional Neural Networks based on Deep Learning. J. Korea Inst. Inf. Commun. Eng. 2 018, 22, 451–457.

17. Sumalee, A.; Ho, H.W. Smarter and more connected: Future intelligent transportation system. Iatss Res. 2018, 42, 67– 71.

18. Veres, M.; Moussa, M. Deep learning for intelligent transportation systems: A survey of emerging trends. IEEE Trans. In tell. Transp. Syst. 2019, 21, 3152–3168.

19. Li, Y.; Wang, H.; Dang, L.M.; Nguyen, T.N.; Han, D.; Lee, A.; Jang, I.; Moon, H. A deep learning-based hybrid framewor k for object detection and recognition in autonomous driving. IEEE Access 2020, 8, 194228–194239.

20. Yahata, S.; Onishi, T.; Yamaguchi, K.; Ozawa, S.; Kitazono, J.; Ohkawa, T.; Yoshida, T.; Murakami, N.; Tsuji, H. A hybrid machine learning approach to automatic plant phenotyping for smart agriculture. In Proceedings of the 2017 Internation al Joint Conference on Neural Networks (IJCNN), Anchorage, AK, USA, 14–19 May 2017; IEEE: Piscataway, NJ, USA, 2017; pp. 1787–1793.

21. Boukhris, L.; Abderrazak, J.B.; Besbes, H. Tailored Deep Learning based Architecture for Smart Agriculture. In Proceed ings of the 2020 International Wireless Communications and Mobile Computing (IWCMC), Limassol, Cyprus, 15–19 Ju ne 2020; IEEE: Piscataway, NJ, USA, 2020; pp. 964–969.

22. Wu, D.; Lv, S.; Jiang, M.; Song, H. Using channel pruning-based YOLO v4 deep learning algorithm for the real-time and accurate detection of apple flowers in natural environments. Comput. Electron. Agric. 2020, 178, 105742.

23. Melenbrink, N.; Rinderspacher, K.; Menges, A.; Werfel, J. Autonomous anchoring for robotic construction. Autom. Const r. 2020, 120, 103391.

24. Lee, D.; Kim, M. Autonomous construction hoist system based on deep reinforcement learning in high-rise building con struction. Autom. Constr. 2021, 128, 103737.

25. Tan, Y.; Cai, R.; Li, J.; Chen, P.; Wang, M. Automatic detection of sewer defects based on improved you only look once algorithm. Autom. Constr. 2021, 131, 103912.

26. Redmon, J.; Divvala, S.; Girshick, R.; Farhadi, A. You only look once: Unified, real-time object detection. In Proceeding s of the IEEE Conference on Computer Vision and Pattern Recognition, Honolulu, HI, USA, 21–26 July 2016; pp. 779– 788.

27. Liu, W.; Anguelov, D.; Erhan, D.; Szegedy, C.; Reed, S.; Fu, C.-Y.; Berg, A.C. Ssd: Single shot multibox detector. In Pro ceedings of the European Conference on Computer Vision, Munich, Germany, 8–14 September 2016; Springer: Berlin/ Heidelberg, Germany, 2016; pp. 21–37.

28. Law, H.; Deng, J. Cornernet: Detecting objects as paired keypoints. In Proceedings of the European Conference on Co mputer Vision (ECCV), Munich, Germany, 8–14 September 2018; pp. 734–750.

29. Lin, T.-Y.; Goyal, P.; Girshick, R.; He, K.; Dollár, P. Focal loss for dense object detection. In Proceedings of the IEEE Int ernational Conference on Computer Vision, Venice, Italy, 22–29 October 2017; pp. 2980–2988.

30. Girshick, R. Fast r-cnn. In Proceedings of the IEEE International Conference on Computer Vision, Santiago, Chile, 7–1 3 December 2015; pp. 1440–1448.

31. Ren, S.; He, K.; Girshick, R.; Sun, J. Faster R-CNN: Towards real-time object detection with region proposal networks. I EEE Trans. Pattern Anal. Mach. Intell. 2016, 39, 1137–1149.

32. Dai, J.; Li, Y.; He, K.; Sun, J. R-fcn: Object detection via region-based fully convolutional networks. In Proceedings of th e Advances in Neural Information Processing Systems, Barcelona, Spain, 5–10 December 2016; pp. 379–387.

33. Su, T.-C.; Yang, M.-D.; Wu, T.-C.; Lin, J.-Y. Morphological segmentation based on edge detection for sewer pipe defect s on CCTV images. Expert Syst. Appl. 2011, 38, 13094–13114.

34. Su, T.-C.; Yang, M.-D. Application of morphological segmentation to leaking defect detection in sewer pipelines. Sensor s 2014, 14, 8686–8704.

35. Haurum, J.B.; Moeslund, T.B. Sewer-ML: A Multi-Label Sewer Defect Classification Dataset and Benchmark. In Proceedings of the IEEE/CVF Conference on Computer Vision and Pattern Recognition, Nashville, TN, USA, 19–25 June 2021; pp. 13456–13467.
36. Kumar, S.S.; Abraham, D.M.; Jahanshahi, M.R.; Iseley, T.; Starr, J. Automated defect classification in sewer closed circuit television inspections using deep convolutional neural networks. Autom. Constr. 2018, 91, 273–283.
37. Meijer, D.; Scholten, L.; Clemens, F.; Knobbe, A. A defect classification methodology for sewer image sets with convolutional neural networks. Autom. Constr. 2019, 104, 281–298.
38. Xie, Q.; Li, D.; Xu, J.; Yu, Z.; Wang, J. Automatic detection and classification of sewer defects via hierarchical deep learning. IEEE Trans. Autom. Sci. Eng. 2019, 16, 1836–1847.
39. Li, D.; Cong, A.; Guo, S. Sewer damage detection from imbalanced CCTV inspection data using deep convolutional neural networks with hierarchical classification. Autom. Constr. 2019, 101, 199–208.
40. Ye, X.; Zuo, J.; Li, R.; Wang, Y.; Gan, L.; Yu, Z.; Hu, X. Diagnosis of sewer pipe defects on image recognition of multi-features and support vector machine in a southern Chinese city. Front. Environ. Sci. Eng. 2019, 13, 17.
41. Hassan, S.I.; Dang, L.M.; Mehmood, I.; Im, S.; Choi, C.; Kang, J.; Park, Y.-S.; Moon, H. Underground sewer pipe condition assessment based on convolutional neural networks. Autom. Constr. 2019, 106, 102849.
42. Dang, L.M.; Kyeong, S.; Li, Y.; Wang, H.; Nguyen, T.N.; Moon, H. Deep Learning-based Sewer Defect Classification for Highly Imbalanced Dataset. Comput. Ind. Eng. 2021, 161, 107630.
43. Myrans, J.; Kapelan, Z.; Everson, R. Automatic identification of sewer fault types using CCTV footage. EPiC Ser. Eng. 2018, 3, 1478–1485.
44. Yin, X.; Chen, Y.; Zhang, Q.; Bouferguene, A.; Zaman, H.; Al-Hussein, M.; Russell, R.; Kurach, L. A neural network-based application for automated defect detection for sewer pipes. In Proceedings of the 2019 Canadian Society for Civil Engineering Annual Conference, CSCE 2019, Montreal, QC, Canada, 12–15 June 2019.
45. Cheng, J.C.; Wang, M. Automated detection of sewer pipe defects in closed-circuit television images using deep learning techniques. Autom. Constr. 2018, 95, 155–171.
46. Wang, M.; Kumar, S.S.; Cheng, J.C. Automated sewer pipe defect tracking in CCTV videos based on defect detection and metric learning. Autom. Constr. 2021, 121, 103438.
47. Wang, M.; Luo, H.; Cheng, J.C. Towards an automated condition assessment framework of underground sewer pipes based on closed-circuit television (CCTV) images. Tunn. Undergr. Space Technol. 2021, 110, 103840.
48. Wang, M.; Cheng, J.C. A unified convolutional neural network integrated with conditional random field for pipe defect segmentation. Comput.-Aided Civ. Infrastruct. Eng. 2020, 35, 162–177.
49. Pan, G.; Zheng, Y.; Guo, S.; Lv, Y. Automatic sewer pipe defect semantic segmentation based on improved U-Net. Autom. Constr. 2020, 119, 103383.
50. Rao, A.S.; Nguyen, T.; Palaniswami, M.; Ngo, T. Vision-based automated crack detection using convolutional neural networks for condition assessment of infrastructure. Struct. Health Monit. 2021, 20, 2124–2142.
51. Chow, J.K.; Su, Z.; Wu, J.; Li, Z.; Tan, P.S.; Liu, K.-f.; Mao, X.; Wang, Y.-H. Artificial intelligence-empowered pipeline for image-based inspection of concrete structures. Autom. Constr. 2020, 120, 103372.
52. Wu, W.; Liu, Z.; He, Y. Classification of defects with ensemble methods in the automated visual inspection of sewer pipes. Pattern Anal. Appl. 2015, 18, 263–276.
53. Sinha, S.K.; Fieguth, P.W. Neuro-fuzzy network for the classification of buried pipe defects. Autom. Constr. 2006, 15, 73–83.
54. Moselhi, O.; Shehab-Eldeen, T. Classification of defects in sewer pipes using neural networks. J. Infrastruct. Syst. 2000, 6, 97–104.
55. Guo, W.; Soibelman, L.; Garrett, J., Jr. Visual pattern recognition supporting defect reporting and condition assessment of wastewater collection systems. J. Comput. Civ. Eng. 2009, 23, 160–169.
56. Khan, S.M.; Haider, S.A.; Unwala, I. A Deep Learning Based Classifier for Crack Detection with Robots in Underground Pipes. In Proceedings of the 2020 IEEE 17th International Conference on Smart Communities: Improving Quality of Life Using ICT, IoT and AI (HONET), Charlotte, NC, USA, 14–16 December 2020; IEEE: Piscataway, NJ, USA, 2020; pp. 78–81.
57. Heo, G.; Jeon, J.; Son, B. Crack automatic detection of CCTV video of sewer inspection with low resolution. KSCE J. Civ. Eng. 2019, 23, 1219–1227.

58. Myrans, J.; Kapelan, Z.; Everson, R. Using automatic anomaly detection to identify faults in sewers. WDSA/CCWI Joint Conference Proceedings. 2018. Available online: https://ojs.library.queensu.ca/index.php/wdsa-ccw/article/view/12030 (accessed on 20 February 2022).
59. Chen, K.; Hu, H.; Chen, C.; Chen, L.; He, C. An intelligent sewer defect detection method based on convolutional neural network. In Proceedings of the 2018 IEEE International Conference on Information and Automation (ICIA), Wuyishan, China, 11–13 August 2018; IEEE: Piscataway, NJ, USA, 2018; pp. 1301–1306.
60. Hawari, A.; Alamin, M.; Alkadour, F.; Elmasry, M.; Zayed, T. Automated defect detection tool for closed circuit television (cctv) inspected sewer pipelines. Autom. Constr. 2018, 89, 99–109.
61. Oullette, R.; Browne, M.; Hirasawa, K. Genetic algorithm optimization of a convolutional neural network for autonomous crack detection. In Proceedings of the 2004 Congress on Evolutionary Computation (IEEE Cat. No. 04TH8753), Portland, OR, USA, 19–23 June 2004; IEEE: Piscataway, NJ, USA, 2004; pp. 516–521.
62. Li, D.; Xie, Q.; Yu, Z.; Wu, Q.; Zhou, J.; Wang, J. Sewer pipe defect detection via deep learning with local and global feature fusion. Autom. Constr. 2021, 129, 103823.
63. Kumar, S.S.; Wang, M.; Abraham, D.M.; Jahanshahi, M.R.; Iseley, T.; Cheng, J.C. Deep learning–based automated detection of sewer defects in CCTV videos. J. Comput. Civ. Eng. 2020, 34, 04019047.
64. Yang, M.-D.; Su, T.-C. Segmenting ideal morphologies of sewer pipe defects on CCTV images for automated diagnosis. Expert Syst. Appl. 2009, 36, 3562–3573.
65. Guo, W.; Soibelman, L.; Garrett, J., Jr. Automated defect detection for sewer pipeline inspection and condition assessment. Autom. Constr. 2009, 18, 587–596.
66. Kumar, S.S.; Abraham, D.M. A deep learning based automated structural defect detection system for sewer pipelines. In Computing in Civil Engineering 2019: Smart Cities, Sustainability, and Resilience; American Society of Civil Engineers: Reston, VA, USA, 2019; pp. 226–233.